

Model-free simulation approach to molecular diffusion tensors

Guillaume Chevrot, Konrad Hinsén, and Gerald R. Kneller

Citation: *J. Chem. Phys.* **139**, 154110 (2013); doi: 10.1063/1.4823996

View online: <http://dx.doi.org/10.1063/1.4823996>

View Table of Contents: <http://jcp.aip.org/resource/1/JCPSA6/v139/i15>

Published by the [AIP Publishing LLC](#).

Additional information on *J. Chem. Phys.*

Journal Homepage: <http://jcp.aip.org/>

Journal Information: http://jcp.aip.org/about/about_the_journal

Top downloads: http://jcp.aip.org/features/most_downloaded

Information for Authors: <http://jcp.aip.org/authors>



Re-register for Table of Content Alerts

Create a profile.



Sign up today!



Model-free simulation approach to molecular diffusion tensors

Guillaume Chevrot,^{1,2} Konrad Hinsén,^{1,2} and Gerald R. Kneller^{1,2,3,a)}

¹Centre de Biophysique Moléculaire, CNRS, Rue Charles Sadron, 45071 Orléans, France

²Synchrotron Soleil, L'Orme de Merisiers, 91192 Gif-sur-Yvette, France

³Université d'Orléans, Chateau de la Source-Av. du Parc Floral, 45067 Orléans, France

(Received 5 July 2013; accepted 18 September 2013; published online 21 October 2013)

In the present work, we propose a simple model-free approach for the computation of molecular diffusion tensors from molecular dynamics trajectories. The method uses a rigid body trajectory of the molecule under consideration, which is constructed *a posteriori* by an accumulation of quaternion-based superposition fits of consecutive conformations. From the rigid body trajectory, we compute the translational and angular velocities of the molecule and by integration of the latter also the corresponding angular trajectory. All quantities can be referred to the laboratory frame and a molecule-fixed frame. The 6×6 diffusion tensor is computed from the asymptotic slope of the tensorial mean square displacement and, for comparison, also from the Kubo integral of the velocity correlation tensor. The method is illustrated for two simple model systems – a water molecule and a lysozyme molecule in bulk water. We give estimations of the statistical accuracy of the calculations. © 2013 AIP Publishing LLC. [<http://dx.doi.org/10.1063/1.4823996>]

I. INTRODUCTION

Anisotropic molecular diffusion plays an essential role in many physicochemical processes and in medical imaging. Such an anisotropy may be caused by the environment in which the molecule under consideration diffuses or by the form of the molecule itself. An example for the first case is the diffusion of water molecules in anisotropic cell tissues probed by magnetic resonance imaging.^{1,2} Intrinsic anisotropic diffusion plays a role in protein aggregation, protein-enzyme encounters,^{3–7} and in the analysis of various spectroscopic experiments. We mention here light scattering,⁸ quasi-elastic neutron scattering,⁹ and nuclear magnetic resonance relaxation spectroscopy.^{10–12}

Molecular dynamics (MD) simulations can contribute valuable insight into anisotropic diffusion processes since they yield a description of molecular dynamics on the atomic scale and allow thus, in principle, an *ab initio* construction of diffusion tensors. In this way, global molecular diffusion can be described in detail which is usually not accessible to experiments. The MD-based diffusion tensors may be subsequently used as input for simulations on coarse-grained time and length scales. Despite these evident advantages, there are not many molecular dynamics studies of anisotropic diffusion of complex molecules. Only recently, a systematic study on that subject has been published.¹³ Here, the principal components (eigenvalues) of the rotational diffusion tensor in the molecular frame are obtained by fitting simulated reorientational correlation times for an ensemble of randomly chosen unit vectors in the molecular frame with an analytical expression containing these principal components. The method is based on the assumption of small rotational anisotropy and an implementation can be found in Ref. 14.

The idea of this paper is to use a straightforward generalization of the computation of translational diffusion coefficients, computing instead of a scalar mean-square displacement the 6×6 mean-square diffusion tensor from the roto-translational trajectory of the molecule under consideration and extracting the components of the diffusion tensor from the asymptotic slope of its time-dependent components. If the molecule under consideration diffuses in an isotropic system, an inherent anisotropy in its rotational motion can only be revealed in a suitably chosen molecule-fixed frame. In this article, we concentrate on the latter case, considering two simple model systems:

- A water molecule diffusing in bulk water.
- A lysozyme molecule diffusing in bulk water.

The paper is organized as follows. In Secs. II and III, we describe, respectively, the theoretical and algorithmic methods for the construction of diffusion tensors, Sec. IV describes its calculations for the model systems described above, and a résumé is presented in Sec. V.

II. THEORY

A. Eckart frame and angular velocity

In the following, we consider the roto-translational diffusion of a non-spherical molecule diffusing in an isotropic medium. If the molecule has internal degrees of freedom, its shape might slightly change in the course of time and one may define an *average* form with respect to an appropriately defined molecule-fixed frame. The definition of such a frame goes back to Eckart,¹⁵ who considered polyatomic molecules whose internal dynamics is described by harmonic vibrations about the equilibrium positions. Such a limitation is, however, not necessary and a more general definition of an Eckart frame has been recently given in Refs. 16 and 17. The central

^{a)}Electronic mail: gerald.kneller@cnrs-orleans.fr

point is that its rotational motion can be expressed as an accumulation of infinitesimal rotations, each describing the rotation of a “virtual” rigid body which is defined by the instantaneous configuration of the molecule under consideration. The latter follows as closely as possible the real motion of the molecule. During an infinitesimal time interval, the mass-weighted atomic positions of the instantaneous virtual rigid body are obtained from a least-squares fit to the corresponding positions in the real molecule. As described in Ref. 16, this follows from Gauss’ principle of least constraint.¹⁸ The cumulated infinitesimal rigid-body motions describe the dynamics of an accompanying frame which is fixed at the center of mass of the molecule and whose initial orientation can be arbitrarily chosen. Within this paper, this frame is referred to as “molecule-fixed (Eckart) frame.”

In the following, we suppose to know the rotation matrix $\mathbf{R}(t)$ which maps the laboratory-fixed basis vectors $\{\mathbf{e}_i\}$ onto the molecule-fixed basis vectors $\{\boldsymbol{\epsilon}_j(t)\}$ of the Eckart frame ($i, j = 1, 2, 3$). Its elements are given by

$$R_{ij}(t) = \mathbf{e}_i \cdot \boldsymbol{\epsilon}_j(t) \quad (1)$$

and its construction has been described in Ref. 17. A brief summary will be given later. The rigid body trajectory of the molecule with respect to the laboratory-fixed frame is then described by the rotation matrix $\mathbf{R}(t)$ and the center-of-mass trajectory,

$$\mathbf{x}_{CM}(t) = \frac{1}{M} \sum_{\alpha} m_{\alpha} \mathbf{x}_{\alpha}(t), \quad (2)$$

where M is the total mass of the molecule and m_{α} the mass of atom α . The time derivative of $\mathbf{R}(t)$ defines the components of the angular velocity in the laboratory-fixed frame and in the body-fixed Eckart frame through

$$\frac{d\mathbf{R}(t)}{dt} = \boldsymbol{\Omega}(t) \cdot \mathbf{R}(t), \quad (3)$$

$$\frac{d\mathbf{R}(t)}{dt} = \mathbf{R}(t) \cdot \boldsymbol{\Omega}'(t), \quad (4)$$

where $\boldsymbol{\Omega}$ and $\boldsymbol{\Omega}'$ are skew symmetric matrices containing the Cartesian components of the angular velocity in the laboratory frame and in the molecule-fixed Eckart-frame, respectively,

$$\boldsymbol{\Omega}^{(\prime)} = \begin{pmatrix} 0 & -\omega_z^{(\prime)} & \omega_y^{(\prime)} \\ \omega_z^{(\prime)} & 0 & -\omega_x^{(\prime)} \\ -\omega_y^{(\prime)} & \omega_x^{(\prime)} & 0 \end{pmatrix}. \quad (5)$$

In both coordinate systems, the components of the angular velocity and the angular momentum, $\mathbf{L} = \sum_{\alpha} m_{\alpha} \mathbf{r}_{\alpha} \wedge \dot{\mathbf{r}}_{\alpha}$ are related via the well-known expression $\boldsymbol{\theta} \cdot \boldsymbol{\omega} = \mathbf{L}$, where $\boldsymbol{\theta}$ is the tensor of inertia, with components $\theta_{ij} = \sum_{\alpha=1}^N m_{\alpha} (|\mathbf{r}_{\alpha}|^2 \delta_{ij} - r_{\alpha,i} r_{\alpha,j})$. If the molecule under consideration can perform motions about its equilibrium configuration, the latter is, however, also time-dependent in the molecule-fixed Eckart frame.

B. Tensorial mean square displacement and diffusion tensor

For the following considerations, we define a roto-translational velocity combining the Cartesian coordinates of the translational velocity,

$$\mathbf{v}_{CM}(t) = \frac{1}{M} \sum_{\alpha} m_{\alpha} \mathbf{v}_{\alpha}(t), \quad (6)$$

where $\mathbf{v}_{\alpha}(t) = d\mathbf{x}_{\alpha}(t)/dt$, with the angular velocity $\boldsymbol{\omega}(t)$ into a six-dimensional column vector

$$\mathbf{V}(t) = \begin{pmatrix} \mathbf{v}_{CM}(t) \\ \boldsymbol{\omega}(t) \end{pmatrix}. \quad (7)$$

The corresponding components in the co-moving Eckart-frame are obtained by

$$\mathbf{V}'(t) = \begin{pmatrix} \mathbf{R}^T(t) & \mathbf{0} \\ \mathbf{0} & \mathbf{R}^T(t) \end{pmatrix} \cdot \mathbf{V}(t). \quad (8)$$

All formulae derived in the following can be defined for the laboratory frame and the Eckart frame. The prime indicating the latter is here omitted. Defining a roto-translational displacement of the molecule as

$$\boldsymbol{\Delta}(t) = \int_0^t d\tau \mathbf{V}(\tau), \quad (9)$$

the time-dependent tensorial mean square displacement matrix is computed via

$$\mathbf{W}(t) = \langle \boldsymbol{\Delta}(t) \cdot \boldsymbol{\Delta}^T(t) \rangle. \quad (10)$$

Assuming that the velocity correlation matrix is stationary,

$$\langle \mathbf{V}(t_1) \cdot \mathbf{V}^T(t_2) \rangle = \langle \mathbf{V}(t_1 + \tau) \cdot \mathbf{V}^T(t_2 + \tau) \rangle, \quad (11)$$

and introducing the abbreviation

$$\mathbf{C}_{vv}(t) := \langle \mathbf{V}(t) \cdot \mathbf{V}^T(0) \rangle, \quad (12)$$

expression (10) may be cast into the alternative form

$$\mathbf{W}(t) = \int_0^t d\tau (t - \tau) \{ \mathbf{C}_{vv}(\tau) + \mathbf{C}_{vv}^T(\tau) \}. \quad (13)$$

Here, we have performed exactly the same steps as in the derivation of the scalar mean-square displacement for the translational motion of a tagged particle which can be found in textbooks on statistical physics.^{19,20} With these preliminaries, we define the diffusion matrix as

$$\mathbf{D} = \frac{1}{2} \int_0^{\infty} d\tau \{ \mathbf{C}_{vv}(\tau) + \mathbf{C}_{vv}^T(\tau) \}, \quad (14)$$

noting that $\mathbf{C}_{vv}(\tau)$ is not symmetric. Here, we exclude anomalous diffusion, such that the integral (14) yields a matrix with finite entries on the diagonal. Using the definition (14) of the diffusion matrix, it follows from (13) that

$$\mathbf{W}(t) \xrightarrow{t \gg \tau_c} 2 \mathbf{D} t + \mathbf{W}_0, \quad (15)$$

where \mathbf{W}_0 is constant and τ_c is the slowest time scale in the relaxation of the velocity correlation functions. The diffusion matrix may be partitioned as

$$\mathbf{D} = \begin{pmatrix} \mathbf{D}_{TT} & \mathbf{D}_{TR} \\ \mathbf{D}_{RT} & \mathbf{D}_{RR} \end{pmatrix}, \quad (16)$$

where the 3×3 matrices correspond to pure translational, pure rotational, and coupled translational-rotational motions. The translational and rotational diffusion constant, respectively, are defined as

$$D_{\text{trans}} = \text{tr}\{\mathbf{D}_{TT}\}/3, \quad (17)$$

$$D_{\text{rot}} = \text{tr}\{\mathbf{D}_{RR}\}/3. \quad (18)$$

III. NUMERICAL AND ALGORITHMIC APPROACH

A. Molecular dynamics simulations

The reference simulation for liquid water was performed for 511 molecules in a cubic box at 300 K, using version 4.6.1 of the GROMACS package,²¹ with the SPCE force field.²² Coulomb interactions were treated with the Particle-Mesh-Ewald (PME) method,^{23,24} using a cutoff radius of 1 nm for the interactions in direct space, and the integration of the equations of motion was performed with the Velocity-Verlet algorithm using a time step of 1 fs. The system was equilibrated with a 200 ps run in *NVT*- and a subsequent 300 ps simulation run in *NPT*-conditions. The production run was performed for 1 ns in the NVE ensemble, saving all 10^6 configurations for later analysis. Due to the fast librational motions of water, such a dense sampling of the stored trajectory is necessary for an *a posteriori* calculation of the angular velocity of the water molecules.

To compute the diffusion tensor of lysozyme, we performed 10 independent MD simulations of one protein surrounded by 16 462 water molecules in a cubic box of $L = 8.03039$ nm side length. The initial configuration for the heavy atoms was taken from entry 193L of the Brookhaven Protein Data Bank²⁵ (PDB) and hydrogen atoms have been added according to the standard rules of stereochemistry. Each production run was performed for 10 ns and preceded by an equilibration run at ambient temperature and pressure of slightly different length, in order to generate different initial configurations. The simulations were performed with GROMACS 4.5.4, using the AMBER99-SB force field²⁶ for the protein, the SPC/E model for water, and the PME method for the calculation of Coulomb interactions. The equations of motions were integrated using a Leap-Frog scheme with a time step of $\Delta t = 1$ fs. All production runs were performed in the NVE ensemble, storing the configurations every 50 fs for subsequent analysis.

B. Numerical calculation of the diffusion tensor

The calculation of the diffusion tensor starts from a full MD trajectory of the molecule under consideration, $\{\mathbf{x}_\alpha(n)\}$, which is sampled at discrete times $t = n\Delta t$. Here, Δt is the

sampling step of the MD trajectory and $n = 0, 1, \dots, N_t - 1$, where N_t is the number of time frames in the MD trajectory. In the following, the procedure is described step by step, distinguishing between the laboratory and the co-moving Eckart frame.

1. We define $\mathbf{r}_\alpha(t) = \mathbf{x}_\alpha(t) - \mathbf{x}_{CM}(t)$ to be the trajectory of atom α with respect to the center-of-mass in the laboratory frame. The whole MD trajectory is translated such that at $n = 0$, the center of mass of the molecule is located at the origin,

$$\mathbf{x}_{CM}(0) = \mathbf{0}, \quad (19)$$

and oriented such that the tensor of inertia corresponding to the positions $\mathbf{r}_\alpha(0)$ is diagonal.

2. The center-of-mass trajectory describes the translational motion of the molecule,

$$\mathbf{x}_{CM}(n) = \frac{1}{M} \sum_{\alpha} m_{\alpha} \mathbf{x}_{\alpha}(n). \quad (20)$$

3. The trajectory of the rotational motion is described by four quaternion parameters, q_0, q_1, q_2, q_3 , satisfying $q_0^2 + q_1^2 + q_2^2 + q_3^2 = 1$. These parameters are obtained in the following way:

- a. We define $\mathbf{r}_{\alpha}^{\text{int}}(t)$ to be the trajectory of the *internal* atomic motions in the co-moving Eckart frame. The procedure is started by setting

$$\mathbf{r}_{\alpha}^{\text{int}}(0) = \mathbf{r}_{\alpha}(0). \quad (21)$$

The corresponding configurations are shown in Fig. 1 for water and in Fig. 6 for lysozyme.

- b. Stepping through the MD trajectory, we perform a series of quaternion-based superposition fits²⁷ and consecutive coordinate transformations yielding the quaternion trajectory $\mathbf{q}(n)$ and the trajectory of the internal atomic motions,

$$\mathbf{r}_{\alpha}^{\text{int}}(n) \xrightarrow{\text{fit}} \mathbf{r}_{\alpha}(n+1) \quad \text{yields} \quad \boxed{\mathbf{q}(n+1)}, \quad (22)$$

$$\boxed{\mathbf{r}_{\alpha}^{\text{int}}(n+1)} = \mathbf{R}^T(\mathbf{q}(n+1)) \cdot \mathbf{r}_{\alpha}(n+1). \quad (23)$$

Here, $n = 0, \dots, N_t - 1$ and the fits are defined by the condition

$$\begin{aligned} & \frac{1}{M} \sum_{\alpha} m_{\alpha} \|\mathbf{R}(\mathbf{q}(n+1)) \cdot \mathbf{r}_{\alpha}^{\text{int}}(n) - \mathbf{r}_{\alpha}(n+1)\|^2 \\ & = \text{Min.}, \end{aligned} \quad (24)$$

where the minimum is to be computed with respect to the quaternion parameters $\mathbf{q}(n+1)$ and the rotation matrix has the form

$$\mathbf{R}(\mathbf{q}) = \begin{pmatrix} q_0^2 + q_1^2 - q_2^2 - q_3^2 & 2(-q_0q_3 + q_1q_2) & 2(q_0q_2 + q_1q_3) \\ 2(q_0q_3 + q_1q_2) & q_0^2 + q_2^2 - q_1^2 - q_3^2 & 2(-q_0q_1 + q_2q_3) \\ 2(-q_0q_2 + q_1q_3) & 2(q_0q_1 + q_2q_3) & q_0^2 + q_3^2 - q_1^2 - q_2^2 \end{pmatrix}. \quad (25)$$

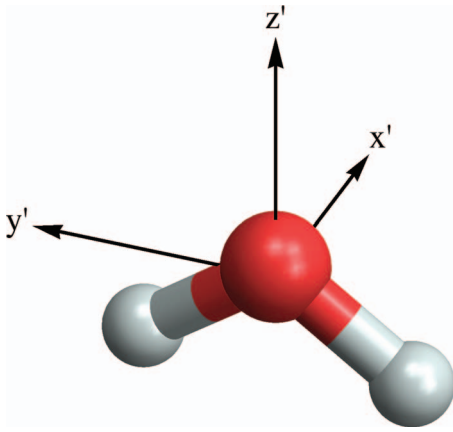


FIG. 1. Orientation of the water molecule in the co-moving Eckart frame.

For more details about the construction of Eckart frames, we refer to Ref. 17.

4. From the center-of-mass, we compute the corresponding time derivative $\mathbf{v}_{CM}(n) = \dot{\mathbf{x}}_{CM}(n)$ using a central difference scheme,

$$\mathbf{v}_{CM}(n) \approx \frac{\mathbf{x}_{CM}(n+1) - \mathbf{x}_{CM}(n-1)}{2\Delta t}. \quad (26)$$

The velocity for the translational motion in the co-moving Eckart frame is then obtained by

$$\mathbf{v}'_{CM}(n) \equiv \mathbf{R}^T(\mathbf{q}(n)) \cdot \mathbf{v}_{CM}(n), \quad n = 0, \dots, N_t. \quad (27)$$

5. The angular velocity $\boldsymbol{\omega}$ is determined in two steps. The first consists in a numerical differentiation of the quaternion trajectory,

$$\dot{\mathbf{q}}(n) \approx \frac{\mathbf{q}(n+1) - \mathbf{q}(n-1)}{2\Delta t}, \quad (28)$$

and the second in the conversion from $\dot{\mathbf{q}}(n)$ to $\boldsymbol{\omega}(n)$. If $\boldsymbol{\omega}(n)$ contains the Cartesian components of the angular velocity in the co-moving Eckart frame, it follows from (3) and (4), respectively, that²⁸

$$\begin{pmatrix} \omega_x \\ \omega_y \\ \omega_z \end{pmatrix} = 2 \begin{pmatrix} -q_1 & q_0 & -q_3 & q_2 \\ -q_2 & q_3 & q_0 & -q_1 \\ -q_3 & -q_2 & q_1 & q_0 \end{pmatrix} \cdot \begin{pmatrix} \dot{q}_0 \\ \dot{q}_1 \\ \dot{q}_2 \\ \dot{q}_3 \end{pmatrix} \quad (29)$$

are the components of the angular velocity in the laboratory frame and that

$$\begin{pmatrix} \omega'_x \\ \omega'_y \\ \omega'_z \end{pmatrix} = 2 \begin{pmatrix} -q_1 & q_0 & q_3 & -q_2 \\ -q_2 & -q_3 & q_0 & q_1 \\ -q_3 & q_2 & -q_1 & q_0 \end{pmatrix} \cdot \begin{pmatrix} \dot{q}_0 \\ \dot{q}_1 \\ \dot{q}_2 \\ \dot{q}_3 \end{pmatrix} \quad (30)$$

are the components of the angular velocity in the body-fixed Eckart frame.

6. From the velocities

$$\mathbf{V}^{(l)}(t) = \begin{pmatrix} \mathbf{v}_{CM}^{(l)}(t) \\ \boldsymbol{\omega}^{(l)}(t) \end{pmatrix}, \quad (31)$$

we construct the displacement trajectory

$$\Delta^{(l)}(t) = \begin{pmatrix} \int_0^t d\tau \mathbf{v}_{CM}^{(l)}(\tau) \\ \int_0^t d\tau \boldsymbol{\omega}^{(l)}(\tau) \end{pmatrix}, \quad (32)$$

computing the integral numerically with a second order Newton-Cotes formula. For the spatial part in the laboratory frame, this step is not explicitly performed since $\mathbf{x}_{CM}(t) = \int_0^t d\tau \mathbf{v}_{CM}(\tau)$ is already given on input.

7. Two approaches are used to compute the diffusion tensor:
 - a. $\mathbf{D}^{(l)}$ is obtained from the asymptotic slope of the components of the tensorial MSD (see Eq. (15)).
 - b. $\mathbf{D}^{(l)}$ is obtained from the Kubo relation (14), using the velocities $\mathbf{V}^{(l)}$ given by Eq. (31). The correlation matrix of the velocities is integrated numerically, using a fixed upper integration limit.

C. Estimation of statistical inaccuracies

The statistical inaccuracy of diffusion tensors for molecules diffusing in an isotropic medium can be estimated by using the fact that in this case \mathbf{D}_{lab} should have the form

$$\mathbf{D}_{lab} = \begin{pmatrix} D_{trans} \mathbf{1} & \mathbf{0} \\ \mathbf{0} & D_{rot} \mathbf{1} \end{pmatrix}, \quad (33)$$

where D_{trans} and D_{rot} are, respectively, the translational and rotational diffusion constant defined through Eqs. (17) and (18). Due to statistical inaccuracies, relation (33) will, of course, not be exactly fulfilled and to quantify the deviation of \mathbf{D}_{lab} from the ideal form we define the 3×3 matrices

$$\delta_{TT} = \mathbf{D}_{lab,TT}^{MD} - D_{trans}^{MD} \mathbf{1}, \quad (34)$$

$$\delta_{RR} = \mathbf{D}_{lab,RR}^{MD} - D_{rot}^{MD} \mathbf{1}, \quad (35)$$

$$\delta_{TR} = \mathbf{D}_{lab,TR}^{MD}, \quad (36)$$

$$\delta_{RT} = \mathbf{D}_{lab,RT}^{MD}, \quad (37)$$

where the superscript ‘‘MD’’ indicates the diffusion tensor obtained from the MD trajectory and

$$D_{trans}^{MD} = \text{tr}\{\mathbf{D}_{lab,TT}^{MD}\}/3, \quad (38)$$

$$D_{rot}^{MD} = \text{tr}\{\mathbf{D}_{lab,RR}^{MD}\}/3, \quad (39)$$

according to (17) and (18). The deviation of each of the matrices δ given in (34)–(37) from the zero matrix are here quantified through the Frobenius norm,

$$\delta = \sqrt{\text{tr}\{\delta^T \cdot \delta\}}, \quad (40)$$

and diffusion tensor elements are considered non-zero only if they fulfill the relation

$$|D_{ij}| > \delta, \quad (41)$$

where the threshold δ is set to δ_{TT} , δ_{RR} , δ_{TR} , or δ_{RT} according to the submatrix to which correspond the indices i, j .

D. Anisotropy

As a scalar measure for the translational and rotational anisotropy, we use

$$\epsilon = \frac{\lambda_{\max} - \lambda_{\min}}{\bar{\lambda}}, \quad (42)$$

where λ_k are the eigenvalues of \mathbf{D}_{TT} or \mathbf{D}_{RR} , respectively, and $\bar{\lambda}$ is the corresponding mean value,

$$\bar{\lambda} = \frac{1}{3}(\lambda_1 + \lambda_2 + \lambda_3). \quad (43)$$

By construction, ϵ is invariant under rotations of the coordinate system and we note that $\bar{\lambda} = D_{\text{trans}}$ or $\bar{\lambda} = D_{\text{rot}}$, depending on which of the two diffusion tensors \mathbf{D}_{TT} or \mathbf{D}_{RR} is considered.

E. Availability of software and data

An ActivePaper²⁹ containing all the software, input datasets, and results from this study is available as the supplementary material.³⁰ The datasets can be inspected with any HDF5-compatible software, e.g., the free HDFView.³¹ Running the programs on different input data requires the ActivePaper software.³² These files also contain plots for all the components of all the correlation functions and mean-square displacements we have computed and of which we show only a selection in this article.

IV. RESULTS

A. Diffusion tensor for SPC/E water

According to the SPC/E model, the simulated water molecules are rigid and the Eckart frame simply follows the *real* rigid body motion of the molecule under consideration. Using the MSD method and averaging over the contributions from all 511 molecules in the system, the diffusion tensor in the laboratory frame is found to be

$$\mathbf{D}_{\text{lab}}^{\text{MSD}} = \left(\begin{array}{ccc|ccc} 2.19 \times 10^{-3} & 0 & 0 & 0 & 0 & 0 \\ 0 & 2.17 \times 10^{-3} & 0 & 0 & 0 & 0 \\ 0 & 0 & 2.17 \times 10^{-3} & 0 & 0 & 0 \\ \hline 0 & 0 & 0 & 2.03 \times 10^{-1} & 0 & 0 \\ 0 & 0 & 0 & 0 & 2.03 \times 10^{-1} & 0 \\ 0 & 0 & 0 & 0 & 0 & 2.04 \times 10^{-1} \end{array} \right), \quad (44)$$

and the Kubo method yields very similar components,

$$\mathbf{D}_{\text{lab}}^{\text{Kubo}} = \left(\begin{array}{ccc|ccc} 2.18 \times 10^{-3} & 0 & 0 & 0 & 0 & 0 \\ 0 & 2.16 \times 10^{-3} & 0 & 0 & 0 & 0 \\ 0 & 0 & 2.15 \times 10^{-3} & 0 & 0 & 0 \\ \hline 0 & 0 & 0 & 2.03 \times 10^{-1} & 0 & 0 \\ 0 & 0 & 0 & 0 & 2.03 \times 10^{-1} & 0 \\ 0 & 0 & 0 & 0 & 0 & 2.04 \times 10^{-1} \end{array} \right). \quad (45)$$

Here, all non-zero elements fulfill the condition (41) and the thresholds for the components in the *TT*, *RR*, *TR*, and *RT* partition, respectively, are resumed in Table I. The same values are used for the calculation of the diffusion tensor in the molecule-fixed frame, which is depicted in Fig. 1. Averaging again over the contributions of all molecules in the simulation box, we find

$$\mathbf{D}_{\text{mol}}^{\text{MSD}} = \left(\begin{array}{ccc|ccc} 3.19 \times 10^{-3} & 0 & 0 & 0 & 6.19 \times 10^{-3} & 0 \\ 0 & 2.03 \times 10^{-3} & 0 & 1.02 \times 10^{-3} & 0 & 0 \\ 0 & 0 & 1.71 \times 10^{-3} & 0 & 0 & 0 \\ \hline 0 & 1.02 \times 10^{-3} & 0 & 1.14 \times 10^{-1} & 0 & 0 \\ 6.19 \times 10^{-3} & 0 & 0 & 0 & 2.1 \times 10^{-1} & 0 \\ 0 & 0 & 0 & 0 & 0 & 2.73 \times 10^{-1} \end{array} \right) \quad (46)$$

with the MSD method and

$$\mathbf{D}_{\text{mol}}^{\text{Kubo}} = \left(\begin{array}{ccc|ccc} 3.21 \times 10^{-3} & 0 & 0 & 0 & 6.30 \times 10^{-3} & 0 \\ 0 & 2.02 \times 10^{-3} & 0 & 1.04 \times 10^{-3} & 0 & 0 \\ 0 & 0 & 1.70 \times 10^{-3} & 0 & 0 & 0 \\ \hline 0 & 1.04 \times 10^{-3} & 0 & 1.14 \times 10^{-1} & 0 & 0 \\ 6.30 \times 10^{-3} & 0 & 0 & 0 & 2.11 \times 10^{-1} & 0 \\ 0 & 0 & 0 & 0 & 0 & 2.72 \times 10^{-1} \end{array} \right) \quad (47)$$

TABLE I. Estimated thresholds for the elements of the diffusion matrix of a SPC/E water molecule. The upper and lower values correspond, respectively, to the Kubo method and the MSD method.

	TT	TR
TT	4.3×10^{-5}	2.2×10^{-4}
	3.7×10^{-5}	2.3×10^{-4}
RT	2.2×10^{-4}	9.4×10^{-4}
	2.3×10^{-4}	1.1×10^{-3}

with the Kubo method, which again leads to very similar components. One recognizes the presence of translational and rotational anisotropies, as well as a significant translation-rotation coupling. The latter indicates preferred screw motions, combining translations along the x -axis with rotations about the y -axis and vice versa.

Figures 2 and 3 show the MSDs for the translational and rotational motion, respectively, along the x , y , z -axes in the molecule-fixed frame (upper part) and in the laboratory frame (lower part). Here, the gray zones indicate the fit intervals for expression (15). The differences clearly indicate an anisotropy for both translational and rotational motions, which is confirmed by looking at the corresponding translational and angular velocity autocorrelation functions depicted in Figs. 4 and 5. Here, the gray regions indicate the integration intervals which have been used to obtain the diffusion tensor by a numerical approximation of the Kubo integral (14).

All relevant parameters are resumed in Table II. The translational diffusion constant is close to the experimental value of $D_{\text{trans}} = 2.4 \times 10^{-3} \text{ nm}^2/\text{ps}$ at 300 K, which is obtained by interpolation from the data in Ref. 33. The rotational diffusion constant is, in contrast, somewhat larger than in experiments. From the Debye relaxation times τ_{rot} published in Ref. 34, we find for 300 K by interpolation $D_{\text{rot}} = 1.27 \times 10^{-1} \text{ ps}^{-1}$, where $D_{\text{rot}} = 1/\tau_{\text{rot}}$. The calculation of hydrodynamic radii has been performed according to

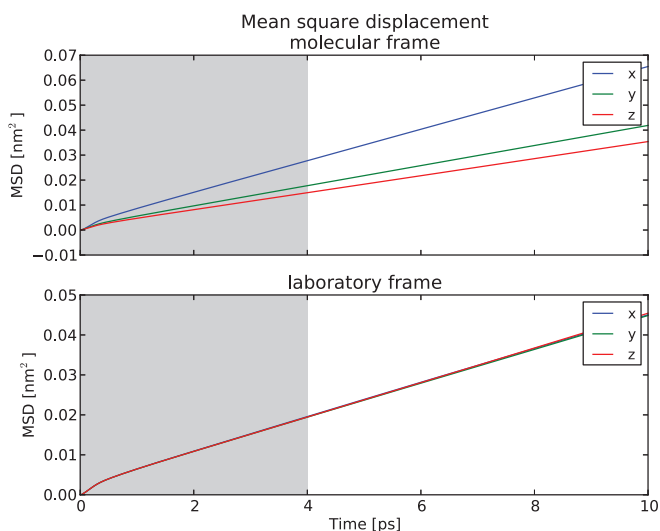


FIG. 2. Diagonal terms of the translational MSD tensor for SPC/E water in the molecule-fixed frame (upper part) and in the laboratory frame (lower part). The gray zone indicates the fit region for expression (15).

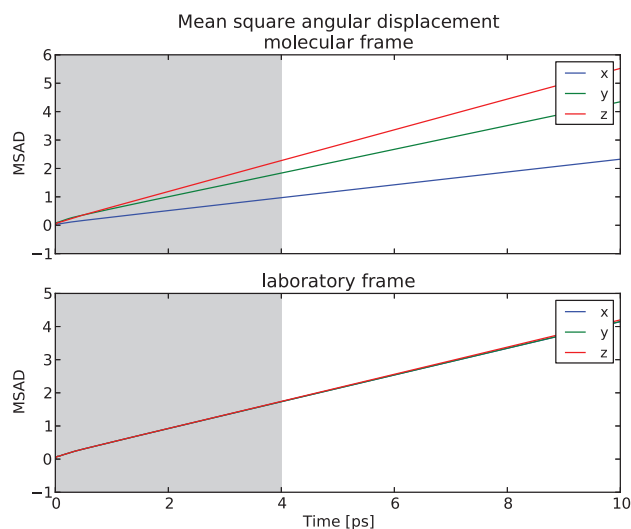


FIG. 3. As Fig. 2, but for the rotational part of the MSD tensor.

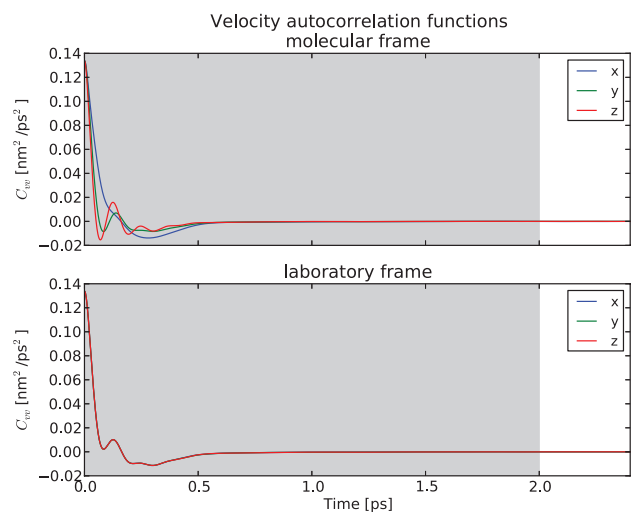


FIG. 4. Diagonal terms of the translational velocity correlation tensor for SPC/E water in the molecule-fixed frame (upper part) and in the laboratory frame (lower part). The gray zone indicates the integration interval for the numerical calculation of expression (14).

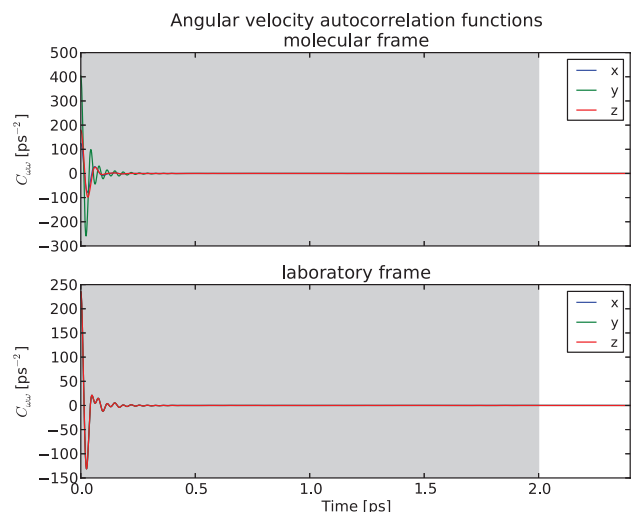


FIG. 5. As Fig. 4, but for the rotational part of the velocity correlation tensor.

TABLE II. Diffusion constants, hydrodynamic radii, and anisotropy parameters for a SPC/E water molecule. The indices “lab” and “mol” refer to the laboratory and molecule-fixed (Eckart) frame and the upper and lower values in each entry to, respectively, the Kubo and the MSD method for the calculation of the diffusion tensor.

	D_t [nm ² /ps]	D_r [1/ps]	a_T [nm]	a_R [nm]	ϵ_T	ϵ_R
Lab	2.16×10^{-3}	2.03×10^{-1}	9.91×10^{-2}	9.25×10^{-2}	2.81×10^{-2}	6.24×10^{-3}
	2.17×10^{-3}	2.03×10^{-1}	9.86×10^{-2}	9.25×10^{-2}	2.38×10^{-2}	7.01×10^{-3}
Mol	2.31×10^{-3}	1.99×10^{-1}	9.29×10^{-2}	9.31×10^{-2}	6.55×10^{-1}	7.97×10^{-1}
	2.31×10^{-3}	1.99×10^{-1}	9.29×10^{-2}	9.32×10^{-2}	6.43×10^{-1}	8.00×10^{-1}

the Stokes-Einstein formulae,

$$D_t = \frac{k_B T}{6\pi\eta a}, \quad (48)$$

$$D_r = \frac{k_B T}{8\pi\eta a^3}. \quad (49)$$

Although it is not evident that a macroscopic hydrodynamic theory can be applied at the scale of a single water molecule, the results of $a \approx 0.09 - 0.1$ nm for both the translational and the rotational hydrodynamic radius are in agreement with the size of a water molecule and demonstrate the consistency of the calculations. The latter is also reflected in the anisotropy parameters, which depend only very little on the method used for the calculation of the diffusion tensor and which show

that the anisotropy in the molecule-fixed frame is statistically significant.

B. Lysozyme

Fig. 6 displays the orientation of the lysozyme molecule in the molecule-fixed Eckart frame which is also the starting configuration of the reoriented MD trajectory. The total size of the MD box is indicated in light blue. As indicated earlier, the diffusion tensor for this molecule was computed by averaging over 10 independent MD simulations, with different initial configurations. Here, the statistical accuracy is clearly less good than in the example for water. Not only the number of independent trajectories is much smaller, but the dynamics is also much slower. Using the MSD approach, we find for the diffusion tensor in the laboratory frame

$$D_{\text{lab}}^{\text{MSD}} = \left(\begin{array}{ccc|ccc} 1.93 \times 10^{-4} & 0 & 0 & 0 & 0 & 0 \\ 0 & 2.07 \times 10^{-4} & 0 & 0 & 0 & 0 \\ 0 & 0 & 1.97 \times 10^{-4} & 0 & 0 & 0 \\ \hline 0 & 0 & 0 & 9.98 \times 10^{-5} & 0 & 0 \\ 0 & 0 & 0 & 0 & 9.94 \times 10^{-5} & 0 \\ 0 & 0 & 0 & 0 & 0 & 1.01 \times 10^{-4} \end{array} \right) \quad (50)$$

which is to be compared to the result of the Kubo method,

$$D_{\text{lab}}^{\text{Kubo}} = \left(\begin{array}{ccc|ccc} 1.92 \times 10^{-4} & 0 & 0 & 0 & 0 & 0 \\ 0 & 2.05 \times 10^{-4} & 0 & 0 & 0 & 0 \\ 0 & 0 & 1.94 \times 10^{-4} & 0 & 0 & 0 \\ \hline 0 & 0 & 0 & 1.03 \times 10^{-4} & 0 & 0 \\ 0 & 0 & 0 & 0 & 9.98 \times 10^{-5} & 0 \\ 0 & 0 & 0 & 0 & 0 & 1.02 \times 10^{-4} \end{array} \right). \quad (51)$$

Again both methods yield almost identical results, but the isotropy for both translational and rotational motion in the laboratory frame is less well established than for the diffusion tensor of water. In this context, we refer to Table III which displays the thresholds which have been computed and used for the components of the diffusion tensor. Using them again in the molecule-fixed frame, we obtain

$$D_{\text{mol}}^{\text{MSD}} = \left(\begin{array}{ccc|ccc} 2.03 \times 10^{-4} & 0 & 0 & 0 & 0 & 0 \\ 0 & 1.99 \times 10^{-4} & 0 & 0 & 0 & 0 \\ 0 & 0 & 1.95 \times 10^{-4} & 0 & 0 & 0 \\ \hline 0 & 0 & 0 & 1.00 \times 10^{-4} & 0 & 0 \\ 0 & 0 & 0 & 0 & 1.07 \times 10^{-4} & 0 \\ 0 & 0 & 0 & 0 & 0 & 9.36 \times 10^{-5} \end{array} \right) \quad (52)$$

with the MSD method and the Kubo method yields

$$D_{\text{mol}}^{\text{Kubo}} = \left(\begin{array}{ccc|ccc} 2. \times 10^{-4} & 0 & 0 & 0 & 0 & 0 \\ 0 & 1.98 \times 10^{-4} & 0 & 0 & 0 & 0 \\ 0 & 0 & 1.91 \times 10^{-4} & 0 & 0 & 0 \\ \hline 0 & 0 & 0 & 1.01 \times 10^{-4} & 0 & 0 \\ 0 & 0 & 0 & 0 & 1.07 \times 10^{-4} & 0 \\ 0 & 0 & 0 & 0 & 0 & 9.69 \times 10^{-5} \end{array} \right). \quad (53)$$

Within the available statistical accuracy, the translational motion is found to be isotropic and for the rotational motion only a very small anisotropy can be detected. The rotation about the molecule-fixed z' -axis is a bit slower than those about the x' - and y' -axes. The coupling of translational and rotational motions can be neglected. The above findings are confirmed by looking at the corresponding MSDs, which are depicted in Figs. 7 and 8. The gray zones indicate again the fit region for expression (15). The first 20 ps are excluded since ballistic effects are here important as a result of the large mass of the lysozyme molecule. One recognizes the parabolic form of $W_{ii}(t) \approx \langle v_{ii}^2 \rangle t^2$ for small times. Although the velocity autocorrelation functions (VACFs) for the translational and rotational motion, which are displayed in Figs. 9 and 10, respectively, do not exhibit any sign of translational or rotational anisotropy, the slight anisotropy for the rotational motion found by the MSD approach is confirmed by the numerical evaluation of the Kubo integral (14). The integration intervals are again indicated by the gray zones.

The essential parameters of the calculations are given in Table IV. The calculations by the MSD and the Kubo method yield again consistent results for the translational and rotational diffusion constants, which are identical in the

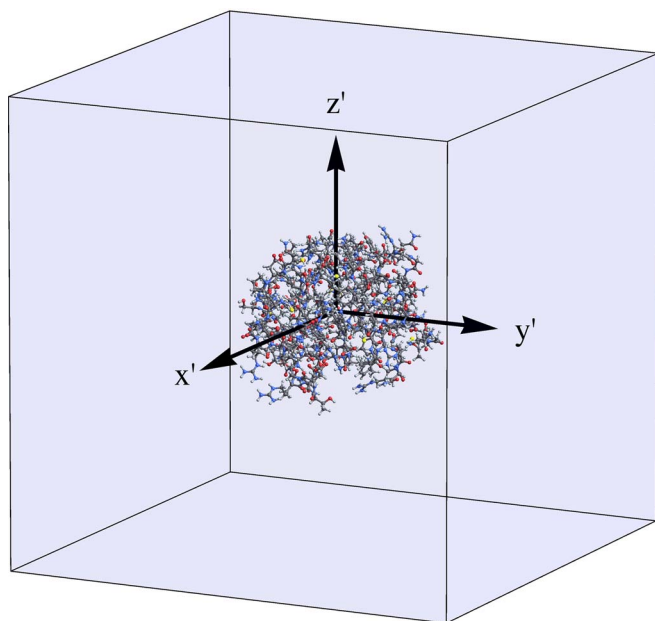


FIG. 6. Ball and stick representation of the lysozyme molecule corresponding to the initial configuration $\{r_{\alpha}^{\text{mol}}(0)\}$ in the Eckart frame. The center-of-mass of the molecule coincides with the center of the MD box, which is given in blue.

laboratory and in the molecule-fixed frame. The fact that the anisotropy parameters are smaller in the molecule-fixed than in the laboratory frame shows that the motional anisotropy is below the statistically relevant threshold and the diffusional motion of the lysozyme molecule must be considered isotropic, as far as the present simulation analysis is concerned. As for the case of water, we obtain similar values for the translational and rotational hydrodynamic radii, which are, however, smaller than the experimental value of $a = 1.77$ nm found by quasielastic light scattering.³⁵

V. RÉSUMÉ

We have presented two approaches for the calculation of molecular diffusion tensors from MD simulations, which are based on the relation between the MSD tensor and the

TABLE III. Estimated thresholds for the elements of the diffusion matrix of a lysozyme molecule. The upper and lower values correspond, respectively, to the Kubo method and the MSD method.

	TT	TR
TT	2.1×10^{-5} 2.3×10^{-5}	7.7×10^{-6} 1.0×10^{-5}
RT	7.7×10^{-6} 1.0×10^{-5}	3.6×10^{-6} 2.9×10^{-6}

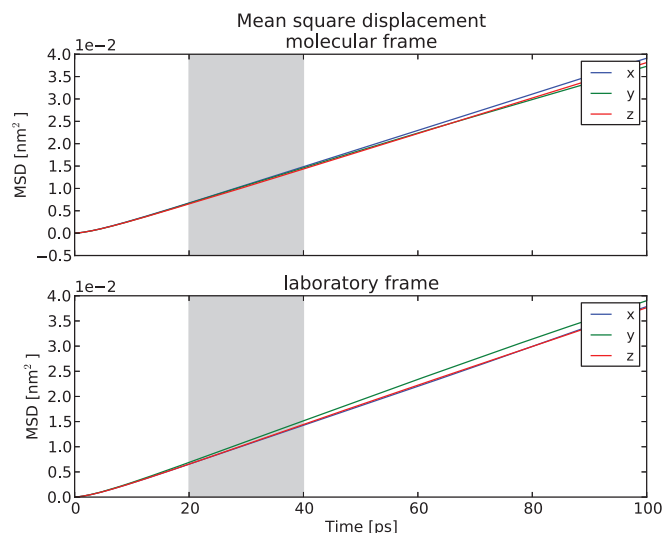


FIG. 7. Diagonal terms of the translational MSD tensor for lysozyme in the molecule-fixed frame (upper part) and in the laboratory frame (lower part). The gray zone indicates the fit region for expression (15).

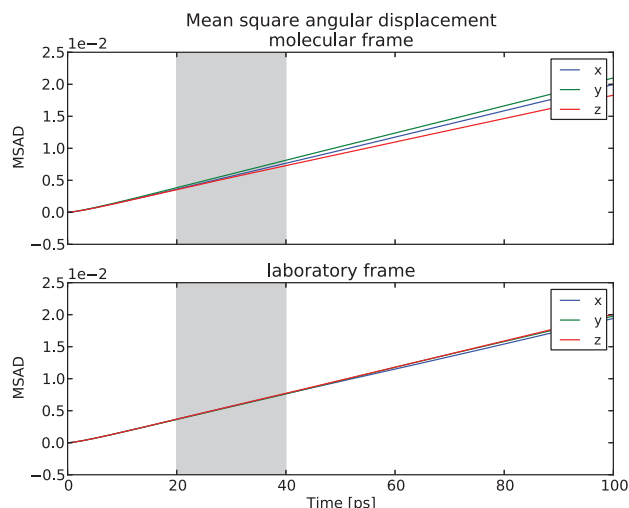


FIG. 8. As Fig. 7, but for the rotational part of the MSD tensor.

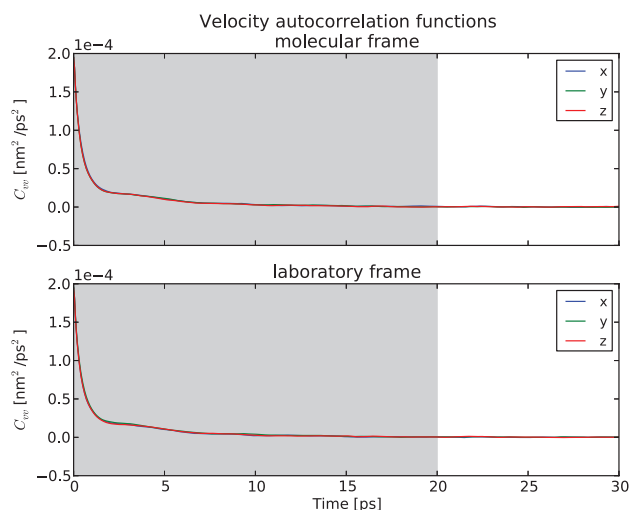


FIG. 9. Diagonal terms of the translational velocity correlation tensor for lysozyme in the molecule-fixed frame (upper part) and in the laboratory frame (lower part). The gray zone indicates the integration interval for the numerical calculation of expression (14).

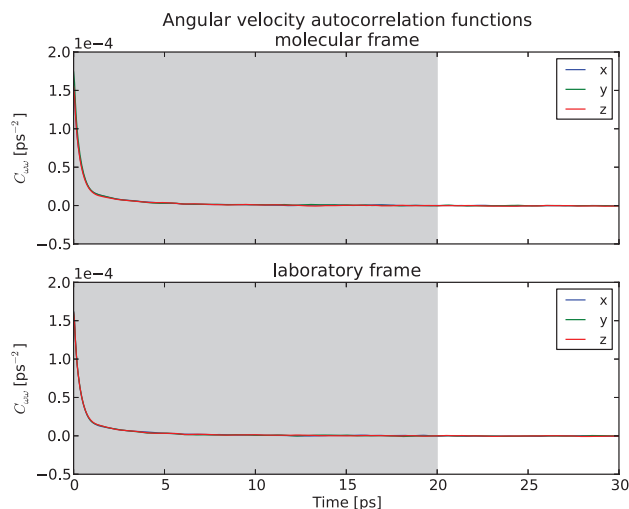


FIG. 10. As Fig. 9, but for the rotational part of the velocity correlation tensor.

TABLE IV. Diffusion constants, hydrodynamic radii, and anisotropy parameters for a lysozyme molecule. The indices “lab” and “mol” refer to the laboratory and molecule fixed (Eckart) frame and the upper and lower values in each entry to, respectively, the Kubo and the MSD method for the calculation of the diffusion tensor.

	D_t [nm ² /ps]	D_r [1/ps]	a_T [nm]	a_R [nm]	ϵ_T	ϵ_R
Lab	1.97×10^{-4}	1.02×10^{-4}	1.09	1.17	1.51×10^{-1}	4.97×10^{-2}
	1.99×10^{-4}	1.00×10^{-4}	1.08	1.17	1.60×10^{-1}	3.96×10^{-2}
Mol	1.97×10^{-4}	1.02×10^{-4}	1.09	1.17	5.43×10^{-2}	1.29×10^{-1}
	1.99×10^{-4}	1.00×10^{-4}	1.08	1.17	5.63×10^{-2}	1.41×10^{-1}

corresponding velocity correlation tensor. In the first case, the diffusion tensor is inferred from the asymptotic slope of the components of the MSD tensor and in the second by Kubo integrals of the corresponding correlation functions. The translational motion is described by the center-of-mass trajectory of the molecule and the angular trajectories are constructed by an accumulation of virtual rigid body motions which are constructed *a posteriori* from a given MD trajectory. For this purpose, we use quaternion-based rigid body fits of consecutive molecular conformations. From the resulting quaternion trajectory, we construct the components of the angular velocity and a subsequent integration yields the angular trajectories of the molecule. From a conceptual point of view, the approach is straightforward and can be considered as a generalization of the usual approaches to compute translational diffusion coefficients. Using 511 rigid SPC/E water molecules in a cubic box as a first test case, we were able to evaluate the reliability of the method, since the molecular diffusion tensor can be averaged over the contributions from all molecules in the box. We found clear anisotropies in the diffusional motion of the water molecules as well as a pronounced translation-rotation coupling. As a second test case, we computed the diffusion tensor for a flexible lysozyme molecule in a cubic water box, averaging the results of ten independent MD simulations. Within the statistical limits, no translation-rotation coupling is observed and the diffusive dynamics is found to be almost isotropic. For both test cases, we find coherent results for the translational and rotational diffusion constants and the corresponding hydrodynamic radii.

ACKNOWLEDGMENTS

Guillaume Chevrot acknowledges financial support from the Agence Nationale de la Recherche, Contract No. ANR-2010-COSI-001-01.

¹P. J. Basser, J. Mattiello, and D. Lebihan, *J. Magn. Reson., Ser. B* **103**, 247 (1994).

²P. Hagmann, L. Jonasson, P. Maeder, J. P. Thiran, V. J. Wedeen, and R. Meuli, *Radiographics* **26**, S205 (2006).

³S. H. Northrup and H. P. Erickson, *Proc. Natl. Acad. Sci. U.S.A.* **89**, 3338 (1992).

⁴J. M. Briggs, *Biophys. J.* **72**, 1915 (1997).

⁵R. R. Gabdouliline and R. C. Wade, *Biophys. J.* **72**, 1917 (1997).

⁶A. Spaar, C. Dammer, R. R. Gabdouliline, R. C. Wade, and V. Helms, *Biophys. J.* **90**, 1913 (2006).

⁷J. Balbo, P. Mereghetti, D. P. Herten, and R. C. Wade, *Biophys. J.* **104**(7), 1576–1584 (2013).

- ⁸B. Berne and R. Pecora, *Dynamic Light Scattering* (Dover Publications, 2000).
- ⁹M. Bée, *Quasielastic Neutron Scattering: Principles and Applications in Solid State Chemistry, Biology and Materials Science* (Adam Hilger, Bristol, 1988).
- ¹⁰A. J. Nederveen and A. M. J. J. Bonvin, *J. Chem. Theory Comput.* **1**, 363 (2005).
- ¹¹E. Meirovitch, Y. E. Shapiro, A. Polimeno, and J. H. Freed, *J. Phys. Chem. A* **110**, 8366 (2006).
- ¹²B. Halle, *J. Chem. Phys.* **131**, 224507 (2009).
- ¹³V. Wong and D. A. Case, *J. Phys. Chem. B* **112**, 6013 (2008).
- ¹⁴D. R. Roe and T. E. Cheatham III, *J. Chem. Theory Comput.* **9**, 3084 (2013).
- ¹⁵C. Eckart, *Phys. Rev.* **47**, 552 (1935).
- ¹⁶G. R. Kneller, *J. Chem. Phys.* **128**, 194101 (2008).
- ¹⁷G. Chevrot, P. Calligari, K. Hinsen, and G. R. Kneller, *J. Chem. Phys.* **135**, 084110 (2011).
- ¹⁸C. Gauß, *J. Reine Angew. Math.* **1829**, 232 (1829).
- ¹⁹J. Boon and S. Yip, *Molecular Hydrodynamics* (McGraw Hill, New York, 1980).
- ²⁰J.-P. Hansen and I. McDonald, *Theory of Simple Liquids*, 2nd ed. (Academic Press, 1986).
- ²¹B. Hess, C. Kutzner, D. van der Spoel, and E. Lindahl, *J. Chem. Theory Comput.* **4**, 435 (2008).
- ²²H. Berendsen, J. R. Grigera, and T. P. Straatsma, *J. Phys. Chem.-US* **91**, 6269 (1987).
- ²³T. Darden, D. York, and L. Pedersen, *J. Chem. Phys.* **98**, 10089 (1993).
- ²⁴U. Essmann, L. Perera, M. L. Berkowitz, T. Darden, H. Lee, and L. G. Pedersen, *J. Chem. Phys.* **103**, 8577 (1995).
- ²⁵J. Kirchmair, P. Markt, S. Distinto, D. Schuster, G. Spitzer, K. Liedl, T. Langer, and G. Wolber, *J. Med. Chem.* **51**, 7021 (2008).
- ²⁶D. A. Case, T. E. Cheatham, T. Darden, H. Gohlke, R. Luo, K. M. Merz, A. Onufriev, C. Simmerling, B. Wang, and R. J. Woods, *J. Comput. Chem.* **26**, 1668 (2005).
- ²⁷G. R. Kneller, *Mol. Simul.* **7**, 113 (1991).
- ²⁸G. R. Kneller, W. Doster, M. Settles, S. Cusack, and J. Smith, *J. Chem. Phys.* **97**, 8864 (1992).
- ²⁹K. Hinsen, *Procedia Comput. Sci.* **4**, 579 (2011).
- ³⁰See supplementary material at <http://dx.doi.org/10.1063/1.4823996> for the software used for the computations and the input and output datasets.
- ³¹The HDF Group, *HDFView*, see <http://www.hdfgroup.org/hdf-java/html/hdfview/>.
- ³²K. Hinsen, *ActivePapers Python edition*, see https://bitbucket.org/khinsen/active_papers_py.
- ³³K. Krynicki, C. D. Green, and D. W. Sawyer, *Faraday Discuss. Chem. Soc.* **66**, 199 (1978).
- ³⁴U. Kaatz, *J. Chem. Eng. Data* **34**, 371 (1989).
- ³⁵B. Nyström and J. Roots, *Makromol. Chem.* **185**, 1441 (1984).